

Unravelling obese black holes in the first galaxies

Bhaskar Agarwal^{1*}, Andrew J. Davis¹ Sadegh Khochfar^{1,3}, Priyamvada Natarajan², James S. Dunlop³

¹Max-Planck-Institut für extraterrestrische Physik, Giessenbachstraße, 85748 Garching, Germany

²Department of Astronomy, 260 Whitney Avenue, Yale University, New Haven, CT, USA

³Institute for Astronomy, University of Edinburgh, Royal Observatory, Edinburgh, EH9 3HJ

00 October 2012

ABSTRACT

We predict the existence and observational signatures of a new class of objects that assembled early, during the first billion years of cosmic time: Obese Black-hole Galaxies (OBGs). OBGs are objects in which the mass of the central black hole initially exceeds that of the stellar component of the host galaxy, and the luminosity from black-hole accretion dominates the starlight. Conventional wisdom dictates that the first galaxies light up with the formation of the first stars; we show here that, in fact, there could exist a population of astrophysical objects in which this is not the case. From a cosmological simulation, we demonstrate that there are sites where star formation is initially inhibited and direct-collapse black holes (DCBHs) form due to the photo-dissociating effect of Lyman-Werner radiation on molecular hydrogen. We show that the formation of OBGs is inevitable, because the probability of finding the required extra-galactic environment and the right physical conditions in a halo conducive to DCBH formation is quite high in the early universe. We estimate an OBG number density of 0.009 Mpc^{-3} at $z \sim 8$ and 0.03 Mpc^{-3} at $z \sim 6$. Extrapolating from our simulation volume, we infer that the most luminous quasars detected at $z \geq 6$ likely transited through an earlier OBG phase. Following the growth history of DCBHs and their host galaxies in an evolving dark matter halo shows that these primordial galaxies start off with an over-massive BH and acquire their stellar component from subsequent merging as well as in-situ star formation. In doing so, they inevitably go through an OBG phase dominated by the accretion luminosity at the Eddington rate or below, released from the growing BH. The OBG phase is characterised by an ultra-violet (UV) spectrum $f_\lambda \propto \lambda^\beta$ with slope of $\beta \sim -2.3$ and the absence of a Balmer Break. OBGs should also be spatially unresolved, and are expected to be brighter than the majority of known high-redshift galaxies. They could also display broad high-excitation emission lines, as expected from Type-I active galactic nuclei (AGN), although the strength of lines such as NV and CIV will obviously depend on the chemical enrichment of the host galaxy. OBGs could potentially be revealed via *Hubble Space Telescope* (HST) follow-up imaging of samples of brighter Lyman-break galaxies provided by wide-area ground-based surveys such as UltraVISTA, and should be easily uncovered and studied with instruments aboard the *James Webb Space Telescope* (JWST). The discovery and characterization of OBGs would provide important insights into the formation of the first black-holes, and their influence on early galaxy formation.

Key words: insert keywords

1 INTRODUCTION

It is now well-established that most present-day galaxies harbour a quiescent super-massive black hole (SMBH), with a mass approximately one thousandth of the mass of stars in the bulge (Ferrarese & Merritt 2000; Häring & Rix 2004). Such a correlation is strongly suggestive of coupled growth of the SMBH

and the stellar component, likely via regulation of the gas supply in galactic nuclei from the earliest times (e.g. Silk & Rees 1998; Haehnelt & Kauffmann 2000; Fabian et al. 2002; King 2003; Thompson et al. 2005; Robertson et al. 2006; Hopkins et al. 2009; Natarajan & Treister 2009; Treister et al. 2011, see however Hirschmann et al. 2010).

Since the same gas reservoir fuels star formation and feeds the black hole, a connection between these two astrophysical processes regulated by the evolving gravitational potential of the dark matter

* E-mail: agarwalb@mpe.mpg.de

halo is arguably expected. However, understanding when and how this interplay commences has been both a theoretical and observational challenge for current theories of structure formation.

In this letter, we explore the formation and evolution of the first massive black-hole seeds and the first stars during the earliest epochs in order to explore the onset of coupling between the black hole and the stellar component. Our calculation incorporates two new physical processes that have only been recently recognised as critical to understanding the fate of collapsing gas in the early universe. The first is the computation of the Lyman-Werner (LW) radiation (11.2 – 13.6 eV) that impacts gas collapse in the first dark-matter haloes (as it is able to efficiently dissociate the H_2 molecules, thereby preventing cooling via molecular hydrogen; e.g. Haiman et al. (2000)). The second is the implementation of our growing understanding of the role of the angular momentum of the baryonic gas in the collapse process (Lodato & Natarajan 2006; Davis & Natarajan 2010). Including these two processes within the context of the standard paradigm of structure formation, predicts the possible existence of a new class of object in the high-redshift Universe in which black-hole growth commences before, and continues to lead the build up of the galaxy stellar population for a significant period of time. We define an OBG as a phase in a galaxy’s evolution where post DCBH formation, the BH at least initially dominates over the stellar mass and is accreting at a rate sufficiently high enough to outshine the stellar component.

OBGs may provide a natural stage of early black-hole/galaxy evolution en route to the most luminous quasars already observed to be in place at $z \simeq 6$ with estimated black-hole masses $M_{\text{BH}} \simeq 10^9 M_{\odot}$. Observationally, such objects should appear similar to moderate-luminosity AGN, but with very low-luminosity host galaxies, and low metallicities.

2 METHODOLOGY

Our model is a modified version of Agarwal et al. (2012), A12 here after, where they identify the sites of DCBH formation by calculating the total amount (spatial and global) of LW radiation seen by any given halo within a cosmological N-body dark-matter only simulation using a semi-analytic model for the star formation in these haloes. The key features of A12 are summarised below:

(i) The DM only N-body simulation is run from $z = 30$ to $z = 6$ with a box size of $\sim 3.4 \text{ Mpc } h^{-1}$ and DM particle mass of $6500 M_{\odot} h^{-1}$. This was chosen so that we can resolve a minimum halo mass $\sim 10^5 M_{\odot}$ with 20 particles, similar to the minimum halo mass that can host a Pop III star at $z = 30$ (Tegmark et al. 1997).

(ii) Both Pop III and Pop II star formation are allowed, and halo histories are tracked in order to determine if a halo is metal free.

(iii) Many realisations of the model are run to study the effect of different LW escape fractions, Pop II star formation efficiencies, gas outflow rates due to supernova feedback, number of Pop III stars forming per halo and reionisation feedback. The results presented here are based on the run with a LW escape fraction of 1.0 and a Pop II star-formation efficiency of 0.005 with a burst mode of star formation. We create Pop II stars in a single burst that is placed randomly between the two time steps for which we use the burst mode template (Fig. 7e) from STARBURST99 (Leitherer et al. 1999). Using the burst mode leads to a peak in LW emission at 10^{-42} erg/s for a 1 Myr old, $10^6 M_{\odot}$ Pop II star cluster which drops to 10^{-38} erg/s at 700 Myr.

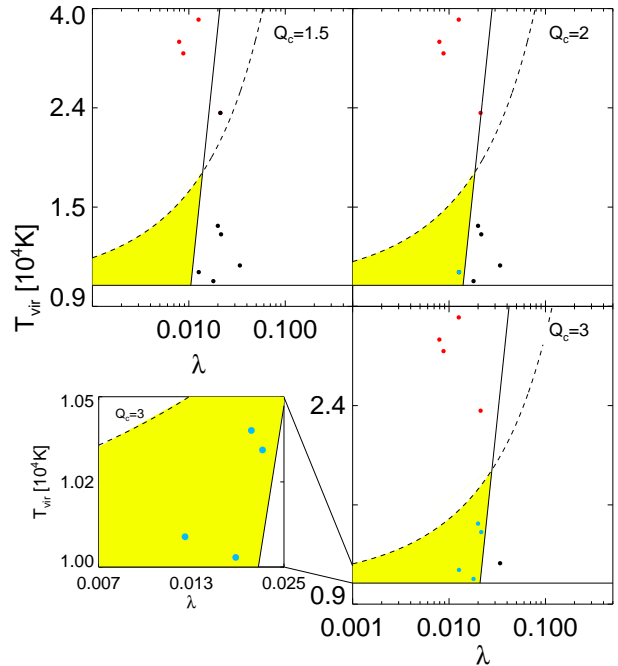


Figure 1. The temperature/spin distribution of pristine massive dark-matter haloes that are exposed to $J_{\text{LW}} \geq J_{\text{crit}}$. The virial temperature, T_{vir} , is plotted against the halo spin parameter, λ , for all DCBH candidates with Toomre stability parameter $Q_c = 1.5, 2, 3$. The nearly-vertical solid curve represents the value of λ_{max} and all haloes with spin less than this critical value lie to the left of this line (red points), whereas those with larger spin lie to the right (black points). The upper limit on the scale-length of the hosted disc given the allowed $T_{\text{vir}} - \lambda_{\text{max}}$ combination is marked as the dashed line. Any halo in the yellow region, i.e. below the dashed line and to the left of the solid vertical curve will host a DCBH (blue points) in our model. Note that the yellow region shrinks as Q_c decreases, thereby reducing the probability of finding a halo that can form a DCBH. Inset: A zoom-in on the $T_{\text{vir}} - \lambda$ distribution of the four DCBH candidates in our fiducial case with $Q_c = 3$.

(iv) The LW specific intensity in units of $10^{-21} \text{ erg s}^{-1} \text{ cm}^{-2} \text{ Hz}^{-1} \text{ sr}^{-1}$, J_{LW} is computed self-consistently depending on the type, mass and age of the stellar population, and with two components: a global and a local contribution. A pristine halo is considered for Pop III star formation or treated as a DCBH candidate depending on the halo’s virial temperature and the J_{LW} that it is exposed to.

(v) The number density of DCBH sites can be up to 0.1 Mpc^{-3} at $z = 6$, much higher than previously anticipated (Dijkstra et al. 2008).

In the present study we refine the model of DCBH formation and also follow the subsequent growth of these seeds as identified in A12. We discuss new additions to the A12 model in the subsections below.

2.1 DCBH forming haloes

A DCBH forms in our model if a pristine massive halo is exposed to $J \geq J_{\text{crit}}^1$ (Wolcott-Green et al. 2011) and satisfies both the spin

¹ Note that J_{crit} is the critical level of LW radiation required by a pristine atomic cooling halo to undergo direct collapse. The critical level of extra-

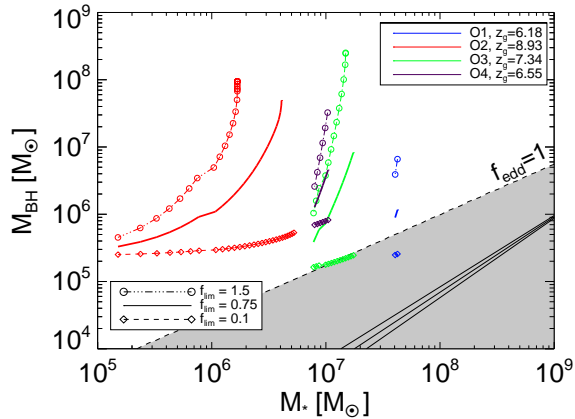


Figure 2. Predicted redshift evolution of M_{BH} and M_* for the four OBGs in our simulation down to $z = 6$. We show the tracks for different fractions of the Eddington accretion rate $f_{\text{lim}} = 1.5, 0.75$ (fiducial), 0.1 . The parameter z_g denotes the redshift when the galaxy becomes an OBG and first appears on this plot. The shaded portion represents the region where the BH’s accretion rate would have to be larger than the Eddington limit for the galaxy to qualify as an OBG. In solid-black lines, we show the local $M_{\text{BH}} - M_{\text{bulge}}$ relation and the $1-\sigma$ error in the fit (Häring & Rix 2004).

and size criterion required for the disc to withstand fragmentation (Lodato & Natarajan 2006, 2007, LN06 and LN07 hereafter). Note that the J_{crit} is always produced by stellar sources external to the pristine DCBH candidate halo as internal sources would pollute the gas inside the halo. We assume the collapsing gas in pristine haloes will settle into a disc whose stability against fragmentation determines whether it will be able to collapse to a BH or will fragment into star-forming clumps (LN06, LN07). Assuming that initially the baryons have the same specific angular momentum as the halo, the halo must have a spin, λ , lower than a characteristic value, λ_{max} , for a given Toomre stability parameter Q_c , for which the pristine gaseous disc is exactly marginally stable and above which no accretion can take place onto the central region (LN06). The critical spin is given as

$$\lambda_{\text{max}} = \frac{m_d^2 Q_c}{8j_d} \sqrt{\frac{T_{\text{gas}}}{T_{\text{vir}}}}, \quad (1)$$

where m_d is the disc mass expressed as a fixed fraction (0.05) of the total baryonic mass in the halo (Mo et al. 1998), j_d is the specific angular momentum of the disc that is also a fixed fraction (0.05) of the halo’s overall angular momentum (LN06), T_{vir} is the virial temperature of the halo and T_{gas} is the temperature of the gas in the disc which depends on whether atomic or molecular hydrogen is the dominant cooling species. In our case, since the halo is exposed to $J \geq J_{\text{crit}}$, the dominant coolant is atomic hydrogen and T_{gas} is set to 8000 K. The second condition comes from the limit that the disc must be cooler than a characteristic temperature above which the gravitational torques required to redistribute the angular momentum become too large and can disrupt the disc. T_{max} is used as a proxy for size of the disc and is defined as

galactic LW radiation required by a pristine atomic cooling halo from Pop III stars, ~ 1000 and from Pop II stars $\sim 30 - 100$ (Wolcott-Green et al. 2011)

$$T_{\text{max}} = T_{\text{gas}} \left(\frac{4\alpha_c}{m_d} \frac{1}{1 + M_{\text{BH}}/m_d M} \right)^{2/3}, \quad (2)$$

where α_c is a dimensionless parameter (0.06) relating the critical viscosity to the gravitational torques in a halo with DM mass, M . This provides a mass estimate for the assembling DCBH (LN07)

$$M_{\text{BH}} = m_d M \left(1 - \sqrt{\frac{8\lambda j_d}{m_d^2 Q_c} \left(\frac{T_{\text{gas}}}{T_{\text{vir}}} \right)^{1/2}} \right), \quad (3)$$

for $\lambda < \lambda_{\text{max}}$ and $T_{\text{vir}} < T_{\text{max}}$.

We find that the inclusion of these two criteria for efficient angular momentum transport and accretion within the disc, in addition to our existing framework for the treatment of LW radiation feedback, fundamentally alters the progression of structure formation in these haloes, and impacts the observable characteristics of stars and the BHs within them.

We plot the $T_{\text{vir}} - \lambda$ distribution of pristine atomic cooling haloes that are exposed to $J_{\text{LW}} \geq J_{\text{crit}}$, for different values of Q_c in Fig. 1. The haloes with spin in the range $\lambda < \lambda_{\text{max}}$ are marked in red, with the almost-vertical solid curve representing λ_{max} , whereas the ones with $\lambda > \lambda_{\text{max}}$ are plotted in black. The size constraint in order for the disc to withstand fragmentation is denoted by the dashed curve. These limits together constrain DCBH formation to a small allowed domain in the $T_{\text{vir}} - \lambda$ plane marked by the yellow region.

Note that LN06, LN07 require the gas disc to be marginally stable i.e. $Q_c \sim O(1)$. Given that the actual high-redshift disc parameters are uncertain, we choose values of Q_c close to unity and use $Q_c = 3$ in our fiducial model, which sets an upper limit on the number of DCBHs with reasonable disc parameters and for which the disc sizes are not too large. This yields DCBHs (blue points) with a co-moving number density of 0.03 Mpc^{-3} in our fiducial case with $Q_c = 3$, and $f_{\text{lim}} = 0.75$ (see the following section for f_{lim}).

2.2 Star Formation

In our model, Pop III stars form in pristine haloes subject to the following physical prescriptions/effects, discussed in A12 in more detail.

- Pop III star formation is prohibited due to LW feedback in pristine haloes with $2000 \leq T_{\text{vir}} < 10^4 \text{ K}$ even when $J_{\text{LW}} < J_{\text{crit}}$ (Machacek et al. 2001; O’Shea & Norman 2008). A pristine minihalo that is subject to even a small value of LW radiation needs to be above a characteristic mass to host a Pop III star due to the partial dissociation (and hence inefficient cooling) of H_2 molecules.

- Pop III stars form following a top-heavy Salpeter IMF with mass limits dependent on halo’s virial temperature, i.e. a single star with mass cut-offs at $[100, 500] M_{\odot}$ in haloes with $2000 \leq T_{\text{vir}} < 10^4 \text{ K}$ and 10 stars with mass cut-offs at $[10, 100] M_{\odot}$ in haloes with $T_{\text{vir}} \geq 10^4 \text{ K}$.

We consider a halo polluted if it has hosted a star or merged with a halo hosting a star. We set a mass threshold of $M > 10^8 M_{\odot}$ for polluted haloes to form Pop II stars (Kitayama et al. 2004; Whalen et al. 2008; Muratov et al. 2012), following the reasoning that a halo needs to be massive enough to allow for the fall back or the retention of metals ejected from a previous Pop III star formation episode. In these polluted haloes, baryons are allowed to co-exist in the form of *hot* non-star-forming gas, *cold* star-forming

gas, stars, or those locked into a DCBH that might have formed in or ended up in the halo through a merger.

We assume in our model that a DM halo is initially comprised of hot gas, $M_{\text{hot}} = f_b M_{\text{DM}}$, where f_b is the universal baryon fraction and M_{DM} is the halo's current DM mass². We add non-star-forming gas to the halo by calculating the accretion rate, \dot{M}_{acc} , defined as

$$\dot{M}_{\text{acc}} \equiv \frac{f_b \Delta M_{\text{DM}} - M_{*,\text{p}} - M_{\text{out,p}} - M_{\text{BH}}}{\Delta t}, \quad (4)$$

In this model ΔM_{DM} is amount by which the DM halo grows between two snapshots separated by Δt years. $M_{*,\text{p}}$ and $M_{\text{out,p}}$ represents the total stellar mass and net mass lost (from both cold and hot gas reservoir) in previous SN outflows at the beginning of the time step, respectively. M_{BH} is the total mass of the DCBH in the halo.

The hot gas, M_{hot} , converts into cold gas, M_{cold} , by collapsing over the dynamical time³ of the halo, t_{dyn} . Pop II star formation can then occur via a Kennicutt-type relation Kennicutt (1998)

$$\dot{M}_{*,\text{II}} = \frac{\alpha}{0.1 t_{\text{dyn}}} M_{\text{cold}}, \quad (5)$$

where α is the star formation efficiency set to 0.005 (SFE) and the factor $0.1 t_{\text{dyn}}$ is motivated by the angular momentum conservation condition for the central galaxy in a DM halo (Kauffmann et al. 1999; Mo et al. 1998, and see A12 for a descriptions of the parameters used).

In Pop II star forming haloes, the outflow rate due to SN feedback is computed via the relation: $\dot{M}_{\text{out}} = \gamma \dot{M}_{*,\text{II}}$, where $\gamma = \left(\frac{V_c}{V_{\text{out}}}\right)^{-\beta}$ Cole et al. (2000).

We set $V_{\text{out}} = 110 \text{ km s}^{-1}$ and $\beta = -1.74$ resulting in typical values of $\gamma \approx 20$, following the results of the high resolution hydrodynamical simulations of the high redshift Universe (Dalla Vecchia and Khochfar 2013, in prep).

We track the evolution of baryons with the following set of coupled differential equations for the individual baryonic components:

$$\dot{M}_{\text{cold}} = \frac{M_{\text{hot}}}{t_{\text{dyn}}} - \dot{M}_{*,\text{II}} - \dot{M}_{\text{out}} - \dot{M}_{\text{BH,cold}}, \quad (6)$$

$$\dot{M}_{\text{hot}} = \dot{M}_{\text{acc}} - \frac{M_{\text{hot}}}{t_{\text{dyn}}} - \dot{M}_{\text{BH,hot}}. \quad (7)$$

Equations 4, 5, 6 and 7 are solved numerically over 100 smaller time steps between two snapshots.

2.3 Growth of a DCBH

Haloes hosting DCBHs are initially not massive enough and are not polluted enough to lead to Pop II star formation (Schneider et al. 2002). It is reasonable to assume that prior to the introduction of a stellar component, the gas reservoir is still massive enough to feed the central BH. At this stage the accreting DCBH might appear as a mini-quasar, but of essentially zero metallicity. Following this epoch, however, the BH grows by accreting gas available in the halo, unchallenged by any further star formation until Pop II stars start forming in the halo, or until the halo merges with another halo

² Using a lower baryon fraction linearly affects the BH mass and evolution discussed in this work.

³ t_{dyn} is defined as the ratio of the halo's virial radius to the circular velocity defined for the infall mass and infall redshift

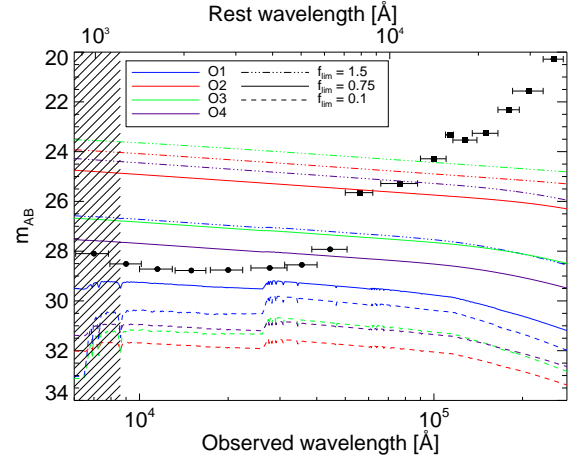


Figure 3. OBG candidates and their observability with JWST at $z \sim 6$. We plot the observed flux density in AB magnitudes for all the OBGs, while varying the maximal allowed accretion rate, f_{lim} . When the BH accretion dominates the spectrum there is virtually no Balmer break, and the UV slope is obviously fixed by the accreting black hole. The black points denote the flux limits and bandpass widths of NIRC2 (circles) and MIRI (squares) wide filters, assuming a 10,000 second exposure with JWST and a S/N ratio of 10. The shaded area marks the wavelength region shortward Ly α , where intergalactic neutral hydrogen is expected to completely absorb the OBG signal.

hosting stars. The stellar component and the BH from this point on begin to grow in tandem, marking the onset of the OBG phase. How the two components evolve in detail is sensitive to the accretion rate and subsequent merging history - a parameter space that we have explored extensively.

Once a DCBH forms in a halo, it is allowed to grow at a fixed fraction f_{lim} of the Eddington accretion rate, assuming that both the cold gas and hot gas can be accreted by the BH. The upper limit of the accretion rate is set by the parameter f_{lim} that we vary between individual runs. If the total gas available during our integration time steps for accretion is less than this fraction, the total mass available sets the accretion rate. We run our model for $f_{\text{lim}} = [1.5, 1.0, 0.75, 0.1]$ to explore the parameter space. From the model, at any given time step, Δt (in Myr), the accretion efficiency computed from the gas reservoir is

$$f_{\text{model}} = \ln(1 + M_g/M_{\text{BH}}) \times \frac{\epsilon}{(1 - \epsilon)} \frac{450 \text{ Myr}}{\Delta t}, \quad (8)$$

where M_g is the total gas available in the halo at timestep Δt and M_{BH} is the DCBH mass with the radiative efficiency, ϵ , set to 10%. The accretion efficiency then used for the actual computation of the increase in the DCBH mass is

$$f_{\text{acc}} = \min[f_{\text{model}}, f_{\text{lim}}], \quad (9)$$

Finally, we write

$$M_{\text{BH,final}} = M_{\text{BH,ini}} \exp\left(f_{\text{acc}} \frac{1 - \epsilon}{\epsilon} \frac{\Delta t}{450 \text{ Myr}}\right), \quad (10)$$

Our fiducial case corresponds to a LW escape fraction of 1.0, Pop II star formation efficiency of 0.005, $Q_c = 3$ and $f_{\text{lim}} = 0.75$. Note that the number of DC sites are directly dependant on f_{esc} and α , where increasing the values of those parameters leads to a higher number of DC sites (A12). The number of DCBHs that form from those sites directly depends on Q_c , where a higher value of Q_c leads to a higher number of DCBHs. The BH accretion pa-

Table 1. Summary of cases considered in our work.

Name	Symbol	Value
Pop II star formation efficiency	α	0.005
LW escape fraction	f_{esc}	1.0
Radiative efficiency	ϵ	0.1
Limiting Eddington Accretion fraction	f_{lim}	0.1-1.5
Toomre Parameter	Q_c	1.5-3

rameters only affect the mass accreted by the DCBH as seen in Fig. 2 (see section 3). In haloes which host a DCBH but are not massive enough to form Pop II stars, the gas is assumed to be hot and diffuse (i.e. has not condensed over the dynamical time of the halo). In haloes which host a DCBH and a Pop II stellar component, both the hot and cold phases of gas are assumed to contribute to the accretion process. The total mass accreted by the DCBH is split into hot and cold components depending on the ratio of the hot and the cold gas reservoirs. We do not assume any feedback from the accreting DCBH affecting star formation in the galaxy. We do this to avoid inserting a correlation between the BH and stars by assuming such a feedback loop since the precise nature of accretion and feedback in galactic nuclei is largely unknown at $z > 6$.

To summarise, the total gas mass available for accretion, and hence the total mass accreted by the DCBH, depends on whether Pop II stars are forming in the halo or not. If there is no assembling Pop II stellar component, the DCBH is assumed to accrete from the hot gas reservoir, i.e the limiting accretion efficiency, $f_{\text{acc}}^{\text{hot}}$, is determined via eqs. 8 and 9 using the hot gas (M_{hot} in eq. 8) in the halo.

$$M_{\text{BH,final}} = M_{\text{BH,ini}} \exp\left(f_{\text{acc}}^{\text{hot}} \frac{1 - \epsilon}{\epsilon} \frac{\Delta t}{450 \text{ Myr}}\right), \quad (11)$$

If the halo hosts a Pop II stellar component, the limiting accretion efficiency, $f_{\text{acc}}^{\text{hot+cold}}$, is determined via eqs. 8 and 9 using the hot and cold gas ($M_{\text{hot}} + M_{\text{cold}}$ in eq. 8) in the halo.

$$M_{\text{BH,final}} = M_{\text{BH,ini}} \exp\left(f_{\text{acc}}^{\text{hot+cold}} \frac{1 - \epsilon}{\epsilon} \frac{\Delta t}{450 \text{ Myr}}\right), \quad (12)$$

The net BH mass accreted in a time step, $M_{\text{BH,acc}} = M_{\text{BH,final}} - M_{\text{BH,ini}}$, can then be written as a sum of the hot ($M_{\text{BH,acc}}^{\text{hot}}$) and cold ($M_{\text{BH,acc}}^{\text{cold}}$) components

$$M_{\text{BH,acc}} = M_{\text{BH,acc}}^{\text{hot}} + M_{\text{BH,acc}}^{\text{cold}}, \quad (13)$$

The individual masses are computed as,

$$M_{\text{BH,acc}}^{\text{cold}} = R M_{\text{cold}}, \quad (14)$$

$$M_{\text{BH,acc}}^{\text{hot}} = (1 - R) M_{\text{hot}}, \quad (15)$$

$$(16)$$

where $R = \frac{M_{\text{cold}}}{M_{\text{hot}}}$, if $M_{\text{cold}} < M_{\text{hot}}$, else $R = \frac{M_{\text{hot}}}{M_{\text{cold}}}$. $M_{\text{BH,acc}}^{\text{cold}}$ and $M_{\text{BH,acc}}^{\text{hot}}$ are then used in eq. 6 and 7 to compute the updated hot and cold gas fractions.

3 RESULTS

For $Q_c = 3$, we find four OBGs, named O1–O4, in our simulation box. The stellar and black-hole growth tracks of these OBGs are shown in Fig. 2, colour coded as O1–blue, O2–red, O3–green, O4–purple, respectively. The fiducial case ($f_{\text{lim}} = 0.75$) is marked by the solid curves and the open triangles and circles denote the time–steps at $f_{\text{lim}} = 0.1, 1.5$. The grey shaded region is where the

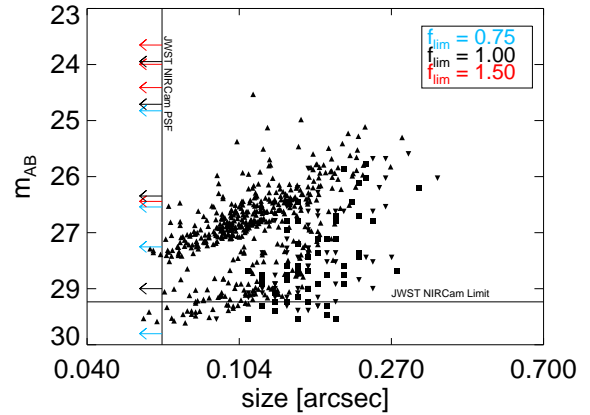


Figure 4. Size versus magnitude relation. The HUDF galaxies, not corrected for point spread function (PSF), at $z = 6, 7, 8$ are represented by up-right triangles, downward triangles and squares respectively. Observational limits and the PSF of the NIRCcam are plotted as the straight lines. The OBGs O1–O4 in our sample, denoted by the arrows pointing left, would be unresolved objects that could be brighter than the galaxies. Note that we have excluded the $f_{\text{lim}} = 0.1$ case from this plot as the m_{AB} for the OBGs is quite high.

BH would need to accrete at super–Eddington rates for the galaxy to appear as an OBG. Since these objects have $M_{\text{BH}} > M_*$, the nuclear emission can dominate the starlight even when accreting at significantly sub–Eddington rates in the non–shaded region.

Note that these OBGs preferably form in low mass atomic cooling haloes as seen in Fig. 1. Almost all the DC candidate haloes meet the spin cut, but only the lower mass haloes, close to $10^7 M_{\odot}$, meet the size cut to allow for the formation of the DCBH. We also report that DCBH host haloes are in fact satellites of larger haloes hosting Pop II stars, in which the DCBH haloes eventually end up. This is, expected as the critical value of the LW radiation is generally produced by the larger star forming haloes forming a close–pair with the DC candidate halo. The abundances of these objects at $z \sim 6$ is similar to the ones reported by Volonteri & Begelman (2010), for their ‘low–threshold’ case of DC seed formation.

3.1 Observational predictions

After identifying the sites of DC (A12), inclusion of physical processes that leads to their formation (LN06), enables the calculation of the observational signatures of OBGs. Haloes that harbour growing DCBH seeds with no (or little) associated stellar component merge into haloes that have formed the first and second generation of stars. We compute the observed spectral energy distribution (SED) of these copiously accreting DCBH seeds and the population of stars within the OBGs. To model the stellar component of the SED, we use the stellar masses and ages from our merger tree and derive the spectrum using STARBURST99 (Leitherer et al. 1999). The accretion disc spectrum is modelled as a radiating blackbody with a temperature profile of the disc given by the alpha–disc model (Pringle 1981). Since OBGs are expected to lie in haloes of low metallicity we do not include any dust absorption in our models. Note that an OBG is characterised by possessing an actively accreting BH and an underlying stellar population that is Pop III or Pop II or both, however an OBG might appear as what has often been

referred to as mini-quasars in the very early stages of its evolution when no stellar component is found in the DCBH host galaxy.

The UV-optical SED of an OBG is inevitably dominated by the accretion onto the central black hole. The predicted SEDs of the OBGs over the wavelength range observable with the NIRCAM (Near Infra-red Camera) and MIRI (Mid-Infra red Instrument) instruments aboard NASA's proposed *James Webb Space Telescope* (JWST) are shown in Fig. 3. The stellar spectrum dominates the OBG spectrum only when the BH is limited to $< 0.1 f_{\text{edd}}$ at all times. However, such a low rate would be incompatible with the dramatic mass growth rates expected of the most massive, early black holes (e.g. Sijacki et al. 2009).

We note that the magnitude of our brightest OBGs could be $m_{\text{AB}} \approx 25$, comparable to the brightest putative Lyman-break galaxies uncovered at $z \approx 7$ in ground-based surveys such as UltraVISTA (Bowler et al. 2012). However, it will be hard to distinguish OBGs from Lyman-break galaxies with ground-based imaging because, while the predicted UV continuum black-hole emission is expected to be relatively blue (with a UV slope $\beta \sim -2.3$, where $f_{\lambda} \propto \lambda^{\beta}$), it is not significantly bluer than that displayed by the general galaxy population at these early times (e.g. Dunlop et al. 2012). OBGs are also of course expected to display a negligible Balmer break. However, while it is interesting that the stack of the brightest Lyman-break galaxies in UltraVISTA shows at most a very weak Balmer break, it will still require extremely high-quality mid-infrared photometry to conclusively rule out the possibility that the UV-optical SED of a putative Lyman-break galaxy is incompatible with that produced by a very young stellar population.

Identification of OBGs amidst the observed high-redshift galaxy population will therefore require high-resolution imaging with HST and ultimately JWST. With $M_{\text{BH}} > M_{*}$, an OBG accreting at a reasonable fraction of the Eddington limit should certainly appear unresolved and point-like in high-resolution rest-frame UV (observed near-infrared) imaging. As illustrated in Fig. 4, it is already known that the vast majority of *faint* high-redshift galaxies uncovered via deep HST imaging are resolved (see Oesch et al. 2010; Ono et al. 2012), but this does not rule out the existence of an OBG population with a surface density $< 1 \text{ arcmin}^{-2}$, and HST follow-up of the brighter and rarer high-redshift ($z \approx 7$) objects uncovered by the near-infrared ground-based surveys is required to establish whether or not they are dominated by central black-hole emission.

4 DISCUSSION AND CONCLUSION

In this study, we report the possible existence of OBGs, at $z > 6$ in which the DCBH precedes the epoch of stellar assembly and outshines the stellar component in for a considerable fraction of the galaxy's lifetime. Our 3.41 Mpc h^{-1} box produces about 4 of these OBGs. Although this is not a cosmological average owing to the small box size, the main aim of this study is to discuss the physical conditions that could lead to the existence of OBGs, which are effects that operate on a scale of less than a few tens of physical kpc, mostly insensitive to our chosen box-size.

Besides the observational features discussed, like all active galactic nuclei, OBGs are expected to display broad-line emission from highly excited species in the vicinity of the black hole. However, as OBGs have very low metallicity, it is unclear whether lines such as NV and CIV are expected to be detectable even given high-quality near-infrared spectroscopy, and Lyman- α is often severely

quenched by neutral Hydrogen as we enter the epoch of reionisation.

Thus, the best observational route to establishing whether OBGs exist, and if so constraining their number density (and ultimately their evolving luminosity function), appears to be via deep imaging of putative high-redshift Lyman-break galaxies, with sufficient angular resolution to prove they are unresolved, coupled with sufficiently accurate photometry to prove any point-like objects cannot be dwarf star contaminants (see, for example Dunlop 2012).

The discovery of an OBG could in principle settle the long standing debate on whether DCBHs can form and be the seeds of the first SMBHs (A12, Dijkstra et al. 2008; Volonteri et al. 2008; Volonteri & Natarajan 2009; Johnson et al. 2012; Bellovary et al. 2011). Uncovering this population holds great promise for understanding the onset of black hole and host galaxy growth.

ACKNOWLEDGEMENTS

The authors would like to thank Rychard Bouwens for providing the HUDF data used in Plot. 4. BA would like to thank Jarrett L. Johnson for his useful comments on the first draft. JSD acknowledges the support of the European Research Council via an Advanced Grant, and the support of the Royal Society through a Wolfson Research Merit award.

REFERENCES

- Agarwal B., Khochfar S., Johnson J. L., Neistein E., Vecchia C. D., Livio M., 2012, MNRAS, 425, 2854
 Bellovary J., Volonteri M., Governato F., Shen S., Quinn T., Wadsley J., 2011, ApJ, 742, 13
 Bowler R. A. A. et al., 2012, MNRAS, 426, 2772
 Cole S., Lacey C. G., Baugh C. M., Frenk C. S., 2000, MNRAS, 319, 168
 Davis A. J., Natarajan P., 2010, MNRAS, 407, 691
 Dijkstra M., Haiman Z., Mesinger A., Wyithe J. S. B., 2008, MNRAS, 391, 1961
 Dunlop J. S., 2012, arXiv: 1205.1543, astro-ph.CO
 Dunlop J. S. et al., 2012, arXiv: 1212.0860, astro-ph.CO
 Fabian A. C., Wilman R. J., Crawford C. S., 2002, MNRAS, 329, L18
 Ferrarese L., Merritt D., 2000, ApJ, 539, L9
 Haehnelt M. G., Kauffmann G., 2000, MNRAS, 318, L35
 Haiman Z., Abel T., Rees M. J., 2000, ApJ, 534, 11
 Häring N., Rix H.-W., 2004, ApJ, 604, L89
 Hirschmann M., Khochfar S., Burkert A., Naab T., Genel S., Somerville R. S., 2010, MNRAS, 407, 1016
 Hopkins P. F., Murray N., Thompson T. A., 2009, MNRAS, 398, 303
 Johnson J. L., Whalen D. J., Holz D. E., 2012, arXiv: 1211.0548, astro-ph.CO
 Kauffmann G., Colberg J. M., Diaferio A., White S. D. M., 1999, MNRAS, 303, 188
 Kennicutt R. C., 1998, ApJ, 498, 541
 King A., 2003, ApJ, 596, L27
 Kitayama T., Yoshida N., Susa H., Umemura M., 2004, ApJ, 613, 631
 Leitherer C. et al., 1999, ApJ, 123, 3
 Lodato G., Natarajan P., 2006, MNRAS, 371, 1813
 Lodato G., Natarajan P., 2007, MNRAS: Letters, 377, L64

- Machacek M. E., Bryan G. L., Abel T., 2001, *ApJ*, 548, 509
Mo H. J., Mao S., White S. D. M., 1998, *MNRAS*, 295, 319
Muratov A. L., Gnedin O. Y., Gnedin N. Y., Zemp M., 2012,
arXiv: 1212.0909
Natarajan P., Treister E., 2009, *MNRAS*, 393, 838
Oesch P. A. et al., 2010, *ApJL*, 709, L21
Ono Y. et al., 2012, arXiv: 1212.3869, 1212, 3869
O’Shea B. W., Norman M. L., 2008, *ApJ*, 673, 14
Pringle J. E., 1981, *Ann. Rev. Astron. Astrophys.*, 19, 137
Robertson B., Hernquist L., Cox T. J., Matteo T. D., Hopkins P. F.,
Martini P., Springel V., 2006, *ApJ*, 641, 90
Sijacki D., Springel V., Haehnelt M. G., 2009, *MNRAS*, 400, 100
Silk J., Rees M. J., 1998, *A&A*, 331, L1
Tegmark M., Silk J., Rees M. J., Blanchard A., Abel T., Palla F.,
1997, *ApJ*, 474, 1
Thompson T. A., Quataert E., Murray N., 2005, *ApJ*, 630, 167
Treister E., Schawinski K., Volonteri M., Natarajan P., Gawiser
E., 2011, *Nature*, 474, 356
Volonteri M., Begelman M. C., 2010, *MNRAS*, 409, 1022
Volonteri M., Lodato G., Natarajan P., 2008, *MNRAS*, 383, 1079
Volonteri M., Natarajan P., 2009, *MNRAS*, 400, 1911
Whalen D., O’Shea B. W., Smidt J., Norman M. L., 2008, *ApJ*,
679, 925
Wolcott-Green J., Haiman Z., Bryan G. L., 2011, *MNRAS*, 1673